Spiral-wave dynamics in excitable medium with excitability modulated by rectangle wave*

Yuan Guo-Yong(袁国勇)[a)b)†]

[a)] *Department of Physics, Hebei Normal University, Shijiazhuang* 050016, *China*

[b)] *Hebei Advanced Thin Films Laboratory, Shijiazhuang* 050016, *China*

(Received 2 November 2010; revised manuscript received 30 December 2010)

We numerically study the dynamics of spiral waves in the excitable system with the excitability modulated by a rectangle wave. The tip trajectories and their variations with the modulation period T are explained by the corresponding spectrum analysis. For a large T, the external modulation leads to the occurrence of more frequency peaks and these frequencies change with the modulation period according to their specific rules, respectively. Some of the frequencies and a primary frequency f_1 determine the corresponding curvature periods, which are locked into rational multiplies of the modulation period. These frequency-locking behaviours and the limited life-span of the frequencies in their variations with the modulation period constitute many resonant entrainment bands in the T axis. In the main bands, which follow the relation $T/T_{12} = m/n$, the size variable R_x of the tip trajectory is a monotonic increasing function of T. The rest of the frequencies are linear combinations of the two ones. Due to the complex dynamics, many unique tip trajectories appear at some certain T. We find also that spiral waves are eliminated when T is chosen from the end of the main resonant bands. This offers a useful method of controling the spiral wave.

Keywords: spiral wave, FitzHugh–Nagumo model, frequency-locking

PACS: 05.45.–a, 05.65.+b, 47.54.–r **DOI:** 10.1088/1674-1056/20/4/040503

1. Introduction

Spiral waves are typical examples of spatiotemporal patterns in macroscopic systems driven far from thermodynamic equilibrium. They exist extensively in excitable and self-oscillating media. For example, cardiac muscle,[1] platinum with oxidation of CO,[2] liquid crystal subjected to electric or magnetic field,[3] the slime mould dictyostelium discoideum,[4] and reacting chemical systems.[5] The dynamics of spiral wave have aroused considerable interest, which is attributed not only to the characteristics of nonlinearity and far-from-equilibrium, but also to its extensive destructions/applications. For example, spiral waves and spatiotemporal chaos from repetitious breakup of spiral waves in cardiac muscle may be the leading mechanism of tachycardia and ventricular fibrillation, respectively. Spiral waves in the brain are believed to be associated with epilepsy. Therefore, there are many "hot" research topics for spiral waves. For example, spiral dynamics, breakup mechanics of spiral waves,[6−8] and controling of spiral waves[9−17] and so on.

The responses of spiral waves to noise, feedback signal and external forcing is another important topic. Fluctuations in excitable media have been used as initiators of new spatial structures,[18−20] where the presence of random perturbations has been found to be necessary for the creation and the sustained maintenance of coherent structures. Noise perturbation can also lead to the occurrence of the transitions and synchronization[21,22] in activator–inhibitor media. The transitions include the appearance of oscillatory behaviours in excitable media and noise-induced excitable behaviours in bistable and oscillatory systems. In the sub-excitable media, optimal amount of noise supports the propagation of structures such as spirals,[23,24] irregular waves,[25,26] traveling pulse,[27] and pulsating spots.[28] Noise can also induce complex spiral dynamics in a simple model of excitable medium.[29,30] In particular, noise may induce turbulent-like states driven by spiral breakup. The types of feedback can be divided into two classes, local feedback and non-local feedback. Under lo-

*Project supported by the National Natural Science Foundation of China (Grant No. 11005030), the Science Foundation of Hebei Education Department, China (Grant No. 2009135), the Science Foundation of Inner Mongolia Education Department, China (Grant No. NJ09178) and the Science Foundation of Hebei Normal University, China.

†Corresponding author. E-mail: g-y-y1975@sohu.com

© 2011 Chinese Physical Society and IOP Publishing Ltd

cal feedback control (known as one-channel feedback) the trajectory of spiral core is attracted to a series of circular limit cycles centred at the measuring point.[31−34] It has been observed that two-channel feedback destroys the regular dynamics seen in one-channel feedback if the measuring points are sufficiently far apart.[35] In the other types of non-local feedback, the modulation is proportional to the integral of the activity in two-dimensional (2D) excitable domains of different shapes[36−41] and on one-dimensional (1D) lines.[42] The nature of the attractors has been examined for circular, square, elliptical, triangle, pentagon and rhombus domains and straight and contour lines. When the domain size and the line size are significantly smaller than the wavelength of the spiral wave, the spiral core trajectories are similar to those for local feedback. However, for larger domains and long lines, the attractors depend significantly on the size and shape of the domain. Spatiotemporal[43] synchronization occurs when the forcing entrains the internal oscillatory dynamics with a sequence of frequency-locked regimes that can be observed as the forcing frequency is varied. A light gradient, which is both rotationally and translationally invariant in space,[44] can induce a resonance drift of a spiral wave. Spiral dynamics under direct current (DC)[45,46] and alternating current (AC)[47] electric fields and periodical mechanical deformations of an elastic excitable medium,[48] also show drift behaviours of vortices.

In this paper, we study numerically the behaviours of spiral waves in the excitable media, whose excitability is modulated by a rectangle wave. The rest of the paper is organized as follows. In Section 2 we describe the mathematical model of the excitable system with the excitable parameter modulated by a rectangle wave. In Section 3 we investigate the dynamics of spiral wave under the modulation. Spiral wave is eliminated for some certain modulation period and the detailed case is studied in Section 4. In Section 5 a discussion and conclusion are presented.

2. Model and method

In our study the FizHugh–Nagumo (FHN) model[49] is used to describe the excitable medium. The FHN model is a set of two-variable "reaction–diffusion" equations. This model is generic for excitable systems and can be applied to a variety of systems. It can reproduce many qualitative characteristics of electrical impulses along nerve and cardiac fibres, such as the existence of an excitation threshold, relative and absolute refractory periods and the generation of pulse trains under the action of external currents. The FHN model reads

$$\frac{\partial u}{\partial t} = \frac{1}{\varepsilon}[-v - u(u-a)(u-1)] + \nabla^2 u, \tag{1}$$

$$\frac{\partial v}{\partial t} = -\gamma v + \beta u - \delta, \tag{2}$$

where variables $u(x,y,t)$ and $v(x,y,t)$, sometimes called activator and inhibitor, describe membrane voltage and v-gate, respectively; ε is the time scale and named excitability parameter; a represents the threshold for excitation; γ, β and δ are parameters controling the rest state and dynamics. Here the parameters $a = 0.03$, $\gamma = 1.0$, $\delta = 0.0$ and $\beta = 2.0$ are fixed. While ε is adjusted by a rectangle wave (shown in Fig. 1) and its values are chosen as follows:

$$\varepsilon = \begin{cases} \varepsilon_1, & \text{if} \quad t \in [nT, nT + T/2), \\ \varepsilon_2, & \text{if} \quad t \in [nT + T/2, (n+1)T), \end{cases} \tag{3}$$

where T is the period of a rectangle wave and $n = 0, 1, 2, 3, \ldots$. In numerical simulations the system Eqs. (1) and (2) are integrated by split operator method with the time step $\Delta t = 0.005$, the space step $h = 0.1$ and a 200×200 array. No-flux condition is chosen. In the following sections, the number of time steps is used as the unit of time unit.

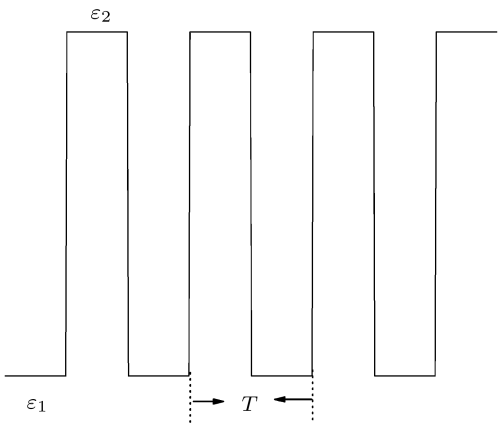


Fig. 1. Excitable parameter modulated by the rectangle wave with period T.

3. Spiral-wave dynamics under rectangle-wave modulation

Switching on a rectangle-wave modulation of the excitable parameter induces complex meandering and drifting spiral waves, which exhibit many special tip

trajectories. We investigate the effect of the modulation period on tip motion by performing numerical simulation of Eqs. (1) and (2) for various values of modulation period T. To study the relation between tip motion and period T, a size variable $R_x = (x_{\max} - x_{\min})/2$, where $x_{\max}$ and $x_{\min}$ are maximum and minimum x-coordinates of the tip orbit respectively, is defined. Figure 2(a) shows R_x as a function of T when $\varepsilon_1 = 0.002$ and $\varepsilon_2 = 0.0046$. The function includes several monotonically increasing parts, which are induced by frequency-locked behaviours. The tip trajectories can be explained by their Fourier spectra. In the Fourier spectra of the x-coordinate time series of the tip, many frequency peaks are exhibited and they are labeled by f_1, f_2, f_3, ..., where f_1 is the frequency with a maximum amplitude between 0.008 and 0.009 (Its value almost does not change with the period of the modulation and it is believed to be the primary rotating frequency of a spiral wave) and the other frequencies f_2, $f_3, \ldots$ follow the order of amplitude from large value to small one. Let $T_1 = 1/f_1$, $T_2 = 1/f_2$ and $T_{12} = 1/(f_1 + f_2)$, which means the main path curvature period of the tip. For several sub-domains on T axis, the modulation period T is close to rational multiples of T_{12}, i.e., $T/T_{12} = m/n$. This indicates that the system locks in the modulation period and the locking region with $T/T_{12} = m/n$ is called as $m : n$ resonant entrainment band with $T/T_{12} = m/n$ (also called as $m : n$ main resonant entrainment band). Several obvious main entrainment bands ($T/T_{12} = 1/1$, $2/1$ and $4/1$) are shown in Fig. 2(b).

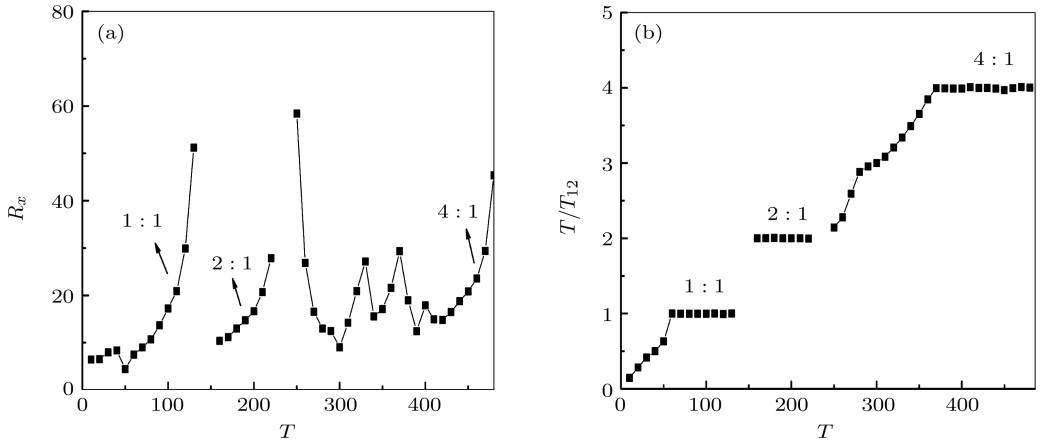


Fig. 2. (a) Variation of size variable R_x with modulation period T. There exist several monotonous increasing parts on the function, which correspond to several main resonant entrainment bands labeled by 1 : 1, 2 : 1 and 4 : 1. (b) T/T_{12} versus modulation period T, where the bands with $T/T_{12} = 1 : 1$, 2 : 1 and 4 : 1 are easily seen. When T is chosen from the discontinuous parts located at the end of the 1 : 1 and 2 : 1 bands, the initial spiral wave in the system is eliminated by the modulation. Here $\varepsilon_1 = 0.002$ and $\varepsilon_2 = 0.0046$.

In the entrainment bands with $T/T_{12} = m/n$, the function $R_x(T)$ is a monotonically increasing one. Figure 3 shows four examples of tip trajectories and the corresponding Fourier spectra in the 1 : 1 band. It is shown that tip trajectories include just one lobe per modulation period T taken from this band. In the 1 : 1 band the frequency f_2 decreases with the increase of T, which results in the increase of large circle radius. In the change the amplitude of f_2 increases. Figure 4 shows four examples of tip trajectories and the corresponding Fourier spectra in the 2 : 1 band.

Figure 5 shows the spectra of tip paths for several different T values between the entrainment bands with $T/T_{12} = 2/1$ and $4/1$. Here the value of f_2 increases with the increase of T, so the entrainment band with $T/T_{12} = m/n$ cannot be constructed. The corresponding amplitude, which is the height of the peak f_2, decreases with the increase of T (shown in Figs. 5(a)–5(e)). When the amplitude decreases to the value lower than the one of f_n ($n > 2$), the old f_2 is replaced by f_n ($n > 2$) and a new f_2 appears (shown in Fig. 5(f)). The new f_2 value decreases with the increase of T and it satisfies the entrainment band with $T/T_{12} = 4/1$. The modulation can also lead to the occurrence of more frequency peaks in tip spectra. In Fig. 5, the frequencies labeled by the same capital letter belong to a family and they satisfy the same varying law. The frequencies marked by the capital letter

A constitute an increasing function of the frequency versus the modulation period T and the frequency value at $T = 250$ approaches zero. While in the B family, the frequency is a decreasing function of T and the modulation period T is four times the path curvature period given by $T_{1A} = 1/(f_A + f_1)$. The frequencies in the C family abide by the law $f_C = 2f_A + f_B$. When $T = 260$, the new frequency f_D is generated according to $T/T_{1D} = 4/1$ (here $T_{1D} = 1/(f_1 + f_D)$), the entrainment band with $T/T_{1D} = 4/1$ is persevered with in the process of increasing T. When T is further increased, the other new families (marked by E, F and G) appear by two mechanisms. For these frequencies labeled by B, D, E and G, they are frequency-locking ($T/T_{1B} = 3/1$, $T/T_{1D} = 4/1$, $T/T_{1E} = 5/1$ and $T/T_{1G} = 6/1$). While for the frequencies labeled by C and F, they are the linear combinations of the corresponding locking frequencies and f_2 ($f_C = 2f_A + f_B$, $f_F = 2f_A + f_G$). We also find the following relation $f_1 = 2f_A + f_D$. In the above definition, the amplitude of f_n ($n > 1$) decreases with the increase of n, so the f_n with the smaller n has a larger effect on the tip path. Here when the frequencies labeled by the same capital letter are described by f_n and the number n changes with T. For example, f_B corresponds to f_3 at $T = 250$, while f_5 at $T = 280$. The detailed frequency-locking relations, exhibited by f_n, are shown in the figure.

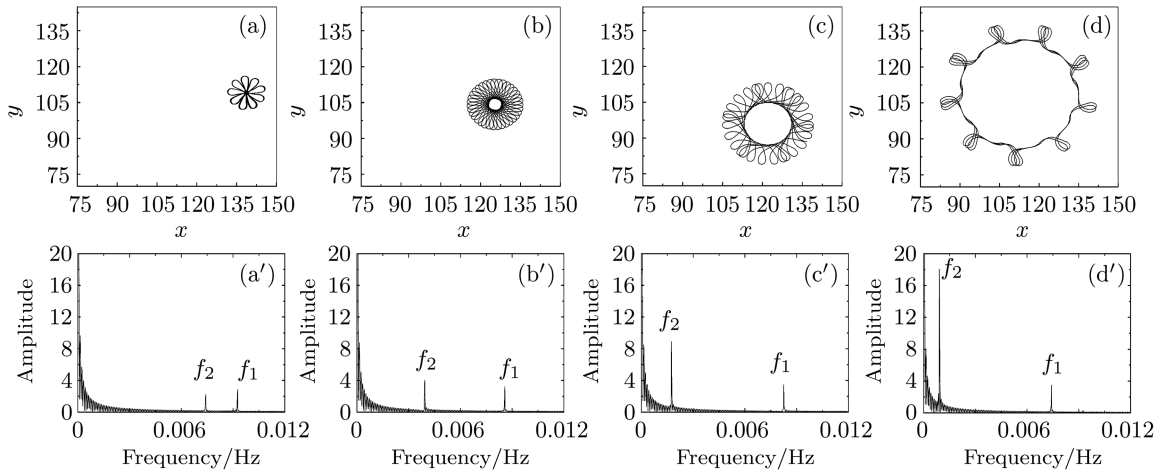


Fig. 3. Four representative tip trajectories on the 1:1 resonant entrainment band ((a)–(d)) and their corresponding Fourier spectra ((a′)–(d′)). (a) (a′) $T = 60$, (b) (b′) $T = 80$, (c) (c′) $T = 100$, (d) (d′) $T = 120$. In the band, the size radius R_x is an increasing function of T. In the corresponding spectrum, the frequency peak f_2 decreases with the increase of T. Here $\varepsilon_1 = 0.002$ and $\varepsilon_2 = 0.0046$.

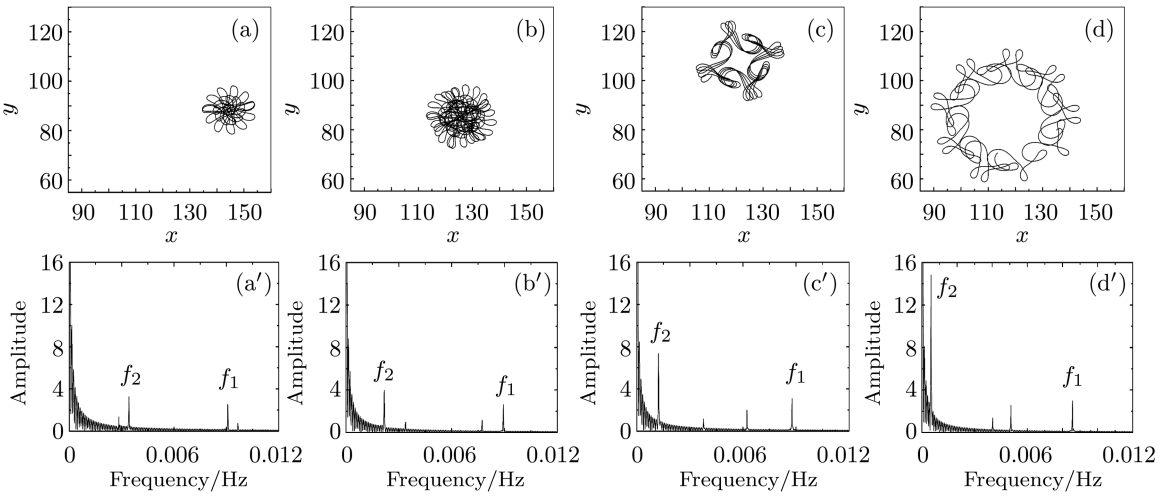


Fig. 4. Four representative tip trajectories on the 2:1 resonant entrainment band ((a)–(d)) and their corresponding Fourier spectra ((a′)–(d′)). (a) (a′) $T = 160$, (b) (b′) $T = 180$, (c) (c′) $T = 200$, (d) (d′) $T = 220$. On the band, the size radius R_x is an increasing function of T. In the corresponding spectra, the frequency peak f_2 decreases with the increase of T. Here $\varepsilon_1 = 0.002$ and $\varepsilon_2 = 0.0046$.

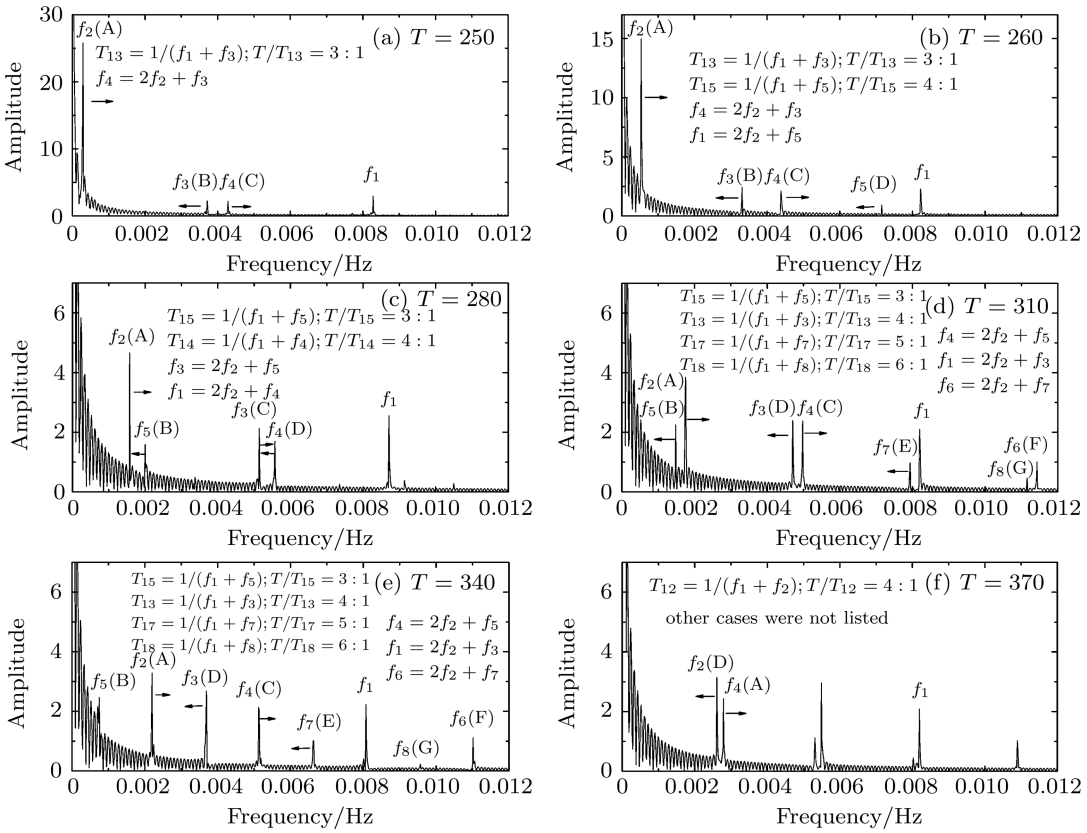
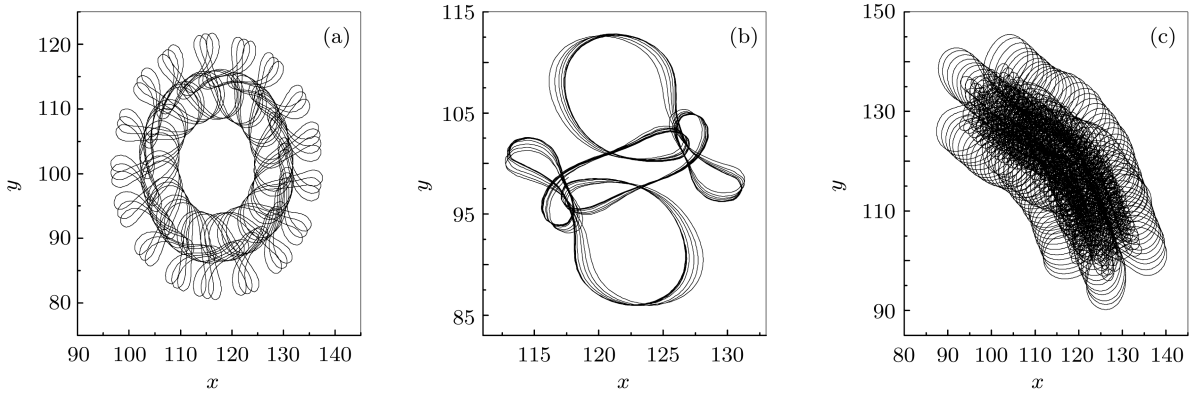


Fig. 5. Fourier spectra of tip paths for six different T values for studying the varying law of tip trajectories with the modulation period between the 2 : 1 and 4 : 1 entrainment bands. Here the peak frequencies are doubly marked by the numerical subscripts $1, 2, 3, \ldots$ and the capital letters A, B, C, ... The heights of the frequency peaks $f_2, f_3, \ldots$ follow the order from small to large. While the frequencies with the same capital letter for different T values constitute a monotonic function of frequency versus the modulation period, which has a different initial value for a different capital letter and they follow the law of the same locking-frequency or linear combination. The variations of frequency peaks with T and kinds of locking-frequency behaviours have been exhibited in the figure. Here $\varepsilon_1 = 0.002$ and $\varepsilon_2 = 0.0046$.

For a large T, more frequency peaks appear in the spectrum of the tip path. In this case, tip patterns become more complex and rich. Figure 6 shows six typical examples of complex tip patterns. The tip path given in Fig. 6(a) shows the coexistence of two types of petals and the corresponding spectrum analysis indicates that the tip motion is dominated by two frequency-locking behaviours ($T/T_{12} = 2/1$ and $T/T_{13} = 3/1$). The patterns, which are not petal orbits or traveling ones, are shown in Figs. 6(b) and 6(f). Figure 6(d) shows a tip pattern consisting of two flowers, the kind of patterns can also drift along a line under several T values (shown in Fig. 6(c)). The tip pattern exhibited by Fig. 6(e) is similar to the tip orbit of modulated traveling waves (MTW) without the periodic modulation, but there exists a great difference between them. Here the tip turns back from the certain locations in the domain, while the tip of MTW returns only from the no-flux boundary.



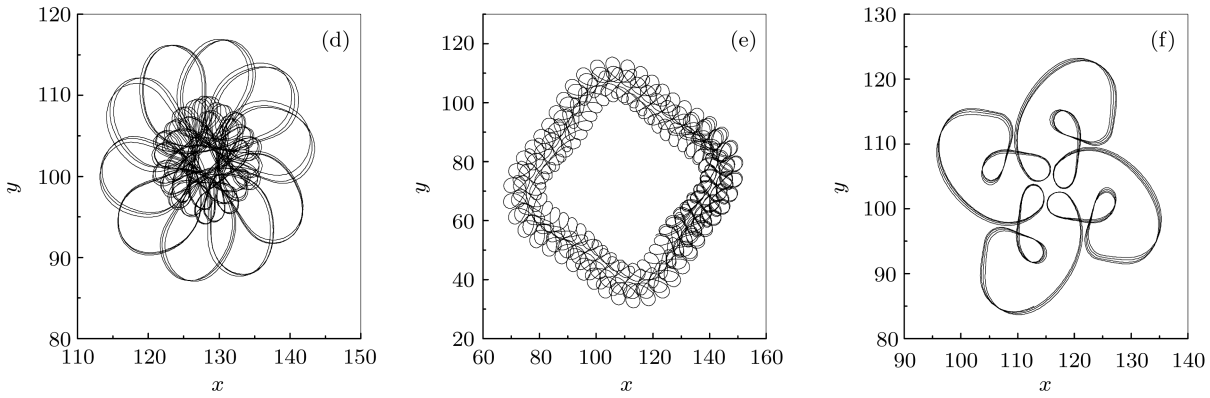


Fig. 6. Six unique patterns of tip trajectories, which are generated due to the appearance of more frequencies and kinds of locking-frequency behaviours with $T = 210$ (a), 300 (b), 320 (c) and 334 (d) with $\varepsilon_1 = 0.002$ and $\varepsilon_2 = 0.0046$ taken in panels (a)–(d), 440 (e) with $\varepsilon_1 = 0.003$ and $\varepsilon_2 = 0.004$ and 320 (f) with $\varepsilon_1 = 0.003$ and $\varepsilon_2 = 0.005$.

4. Eliminating of spiral wave under some modulation periods

We also find that a spiral wave can be eliminated when the value of the modulation period T is taken from the ends of the main entrainment bands. The elimination is generally speedy and it is favoured in a real application. Figure 4 shows the disappearing process of a spiral wave under the parameter modulation. First, the spiral wave core drifts speedily toward the boundary along a straight line. When the tip arrives at the boundary, it is cut off from the body and then the isolated tip disappears gradually from the no-flux boundary.

Here transitive modulated traveling waves (MTW), i.e., solutions whose tip core drifts along a straight line in a laboratory frame (viewed in a co-moving frame, the solutions are quasi-periodic), can be explained by the spectra shown in Figs. 2 and 3. It has been known from the above discussion that the decrease of frequency f_2 results in the increase of large circle radius in the main bands. On the end of the bands f_2 is very close to zero and the value of the large circle radius approaches infinity, so the transitive MTW appears. This is different from the MTW from the Barkley model. In the Barkley model, the MTW state separates the modulated rotating waves (MRW) states with inward petals from those with outward petals. The MRW states with outward petals are such that $f_2 > f_1$ and the states with inward petals are such that $f_2 < f_1$, whereas the MTW states need to satisfy the condition $f_2 = f_1$. There exists another difference between the two kinds of MTW states. For an MTW from the Barkley model, the tip turns back to the domain when it reaches the boundary. While for the transitive MTW from the system Eqs. (1) and (2) with the parameter modulation, the tip disappears when it arrives at the boundary.

5. Discussion and conclusion

In the absence of external modulation the system with the above fixed parameters supports meandering spiral waves with the tips tracing out a flower pattern with outward petals. The motion of the wave is quasi-periodic in the laboratory and time-periodic in a co-rotating frame. The tip motion consists of a large circle rotating at frequency $f^{\rm rot} + kf$ and an $O(1)$ rotation with frequency $f^{\rm rot}$. The rotating wave rotates clockwise and the large circle is traversed by the spiral tip counterclockwise, so that the meandering motion has outward petals. In this case two frequencies are observed in the Fourier spectra of the x-coordinate time series of the tip. External rectangle-wave modulation of the excitable parameter leads to relative invariant tori, i.e., invariant tori of the symmetry reduced dynamics. This is a form of generalized meandering or hyper-meandering. In this case, more frequency peaks appear in the Fourier spectra of the tip path and they can be divided into two groups. The frequencies in the first group are correlated with the modulation frequency $1/T$ by frequency-locking behaviours, while the ones in the second group are generated by the linear combination. These complex nonlinear mechanisms lead to the appearance of more rich tip patterns. The frequency f_1 is the primary rotating frequency of the spiral wave, which can be measured far from the spiral core and it will not disappear when the modulation period T is changed. While the other frequencies have a limited life-span ΔT in the T-axis, i.e., they are generated at a certain T and then disappear at $T + \Delta T$. The birth of the

frequencies is due to the occurrence of a supercritical Hopf bifurcation, while their deaths correspond to the subcritical Hopf bifurcation. So the same type of frequency-locking behaviours can be maintained in many certain ranges for the modulation period T and the certain ranges are called as resonant entrainment bands. In the $T/T_{12} = m/n$ band, the size of tip orbit is a monotonically increasing function of T and it is easy to be explained by spectrum analysis.

Under the rectangle-wave modulation with a certain period T, which lies in the end of the $T/T_{12} = m/n$ band, spiral tip shifts rapidly to the no-flux boundary and then disappears from here. This offers a method for eliminating spiral waves. The drift along a straight line is due to $f_2 \to 0$ and is different from MTW in the Barkey model. In the absence of the parameter modulation, generally, the spiral tip moves along a cycloidal orbit. When the tip with the smooth and regular motion approaches the no-flux boundary, it does not flee away from there. However, this case can occur in the presence of the excitability modulation. From Fig. 7, we see that the tip trajectory includes two elementary units, which correspond respectively to the short straight walk and the small lobe, formed by curling tightly. When the tip arrives at the boundary, there always exists a chance for the modulation to make the tip flee away from the boundary along a unit of straight trip.

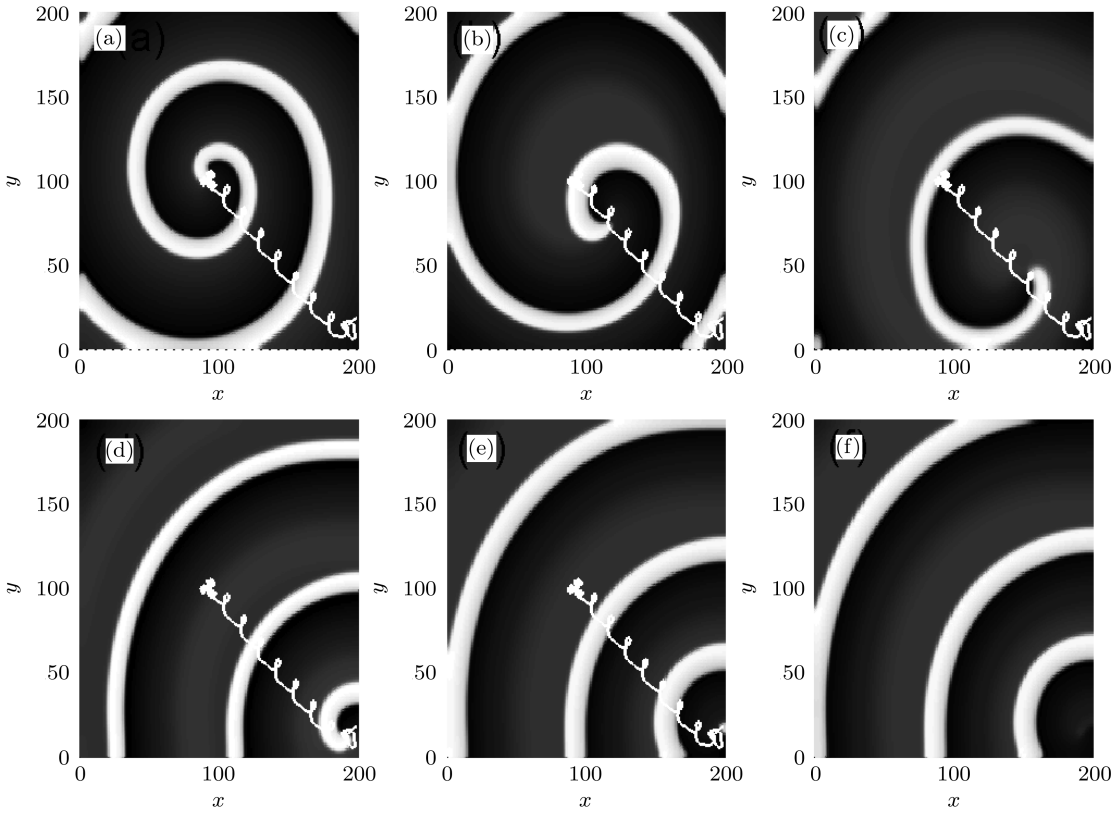


Fig. 7. Eliminated process of the spiral wave with $T = 150$, $\varepsilon_1 = 0.002$ and $\varepsilon_2 = 0.0046$, rectangle-wave modulation of the excitability applied at $t = 0$ and the initial state being a spiral wave, at $t = 5$ (a), 820 (b), 1186 (c), 1758 (d), 1789 (e) and 1797 (f).

References

[1] Courtemanche M 1996 *Chaos* **6** 579

[2] Nettesheim S, Oertzen A V, Rotermund H H and Ertl G 1993 *J. Chem. Phys.* **98** 9977

[3] Frisch T, Rica S, Coullet P and Gilli J M 1994 *Phys. Rev. Lett.* **72** 1471

[4] Van Oss C, Panfilov A V, Hogeweg P, Siegert F and Weijer C J 1996 *J. Theor. Biol.* **181** 203

[5] Winfree A T and Strogatz S H 1983 *Physica* D **8** 35

[6] Ouyang Q, Swinney H L and Li G 2000 *Phys. Rev. Lett.* **84** 1047

[7] Zhou L Q and Ouyang Q 2000 *Phys. Rev. Lett.* **85** 1650

[8] Zhang H, Ruan X S, Hu B and Ouyang Q 2004 *Phys. Rev.* E **70** 016212

[9] Tang G N, Deng M Y, Hu B and Hu G 2008 *Phys. Rev.* E **77** 046217
[10] Wu N J, Zhang H, Ying H P, Cao Z J and Hu G 2006 *Phys. Rev.* E **73** 060901R
[11] Kim M, Bertram M, Pollmann M, Oertzen A, Mikhailov A S, Rotermund H H and Ertl G 2001 *Science* **292** 1357
[12] Sakaguchi H and Fujimoto T 2003 *Phys. Rev.* E **67** 067202
[13] Wang P Y and Xie P 2000 *Phys. Rev.* E **61** 5120
[14] Zhang H, Cao Z, Wu N J, Ying H P and Hu G 2005 *Phys. Rev. Lett.* **94** 188301
[15] Yuan G Y, Wang G R and Chen S G 2005 *Europhys. Lett.* **72** 908
[16] Yuan G Y, Chen S G and Yang S P 2007 *Euro. Phys. J.* B **58** 331
[17] Ma J, Wang C N, Jin W Y, Li Y L and Pu Z S 2008 *Chin. Phys.* B **17** 2844
[18] Wang J, Kádár S, Jung P and Showalter K 1999 *Phys. Rev. Lett.* **82** 855
[19] García-Ojalvo J and Schimansky-Geier L 1999 *Europhys. Lett.* **47** 298
[20] Maselko J and Showalter K 1991 *Physica* D **49** 21
[21] Lindner B, García-Ojalvo J, Neiman A and Schimansky-Geier L 2004 *Phys. Rep.* **392** 321
[22] Sagués F, Sancho J M and García-Ojalvo J 2007 *Rev. Mod. Phys.* **79** 829
[23] Jung P and Mayer-Kress G 1995 *Chaos* **5** 458
[24] Jung P and Mayer-Kress G 1995 *Phys. Rev. Lett.* **74** 2130
[25] Jung P 1997 *Phys. Rev. Lett.* **78** 1723
[26] Jung P, Cornell-Bell A, Madden K and Moss F 1998 *J. Neurophysiol.* **79** 1098
[27] Kádár S, Wang J and Showalter K 1998 *Nature* **391** 770
[28] Hempel H, Schimansky-Geier L and García-Ojalvo J 1999 *Phys. Rev. Lett.* **82** 3713
[29] Winfree A T 1991 *Chaos* **1** 303
[30] Sendiña-Nadal I, Alonso S, Pérez-Muñuzuri V, Gómez-Gesteira M, Pérez-Villar V, Ramírez-Piscina L, Casademunt J, Sancho J M and Sagués F 2000 *Phys. Rev. Lett.* **84** 2734
[31] Steinbock O, Zykov V S and Müller S C 1993 *Nature* **366** 322
[32] Braune M and Engel H 2000 *Phys. Rev.* E **62** 5986
[33] Zykov V S, Kheowan O U, Rangsiman O and Müller S C 2002 *Phys. Rev.* E **65** 026206
[34] Kheowan O U, Zykov V S, Rangsiman O and Müller S C 2001 *Phys. Rev. Lett.* **86** 2170
[35] Zykov V S, Brandtstädter H, Bordiougov G and Engel H 2005 *Phys. Rev.* E **72** 065201R
[36] Zykov V S, Bordiougov G, Brandtstädter H, Gerdes I and Engel H 2004 *Phys. Rev. Lett.* **92** 018304
[37] Zykov V S and Engel H 2004 *Phys. Rev.* E **70** 016201
[38] Kheowan O U, Kantrasiri S, Wilairat P, Storb U and Müller S C 2004 *Phys. Rev.* E **70** 046221
[39] Kheowan O U, Kantrasiri S, Uthaisar C, Gáspár V and Müller S C 2004 *Chem. Phys. Lett.* **389** 140
[40] Naknaimueang S, Allen M A and Müller S C 2006 *Phys. Rev.* E **74** 066209
[41] Zykov V S and Engel H 2004 *Physica* D **199** 243
[42] Yuan G Y, Xu A G, Wang G R and Chen S G 2010 *Europhys. Lett.* **90** 10013
[43] Braune M and Engel H 1993 *Chem. Phys. Lett.* **211** 534
[44] Markus M, Nagy-Ungvarai Z and Hess B 1992 *Science* **257** 225
[45] Steinbock O, Schütze J and Müller S C 1992 *Phys. Rev. Lett.* **68** 248
[46] Agladze K I and De Kepper P 1992 *J. Phys. Chem.* **96** 5239
[47] Muñuzuri A P, Gómez-Gesteira M, Pérez-Muñuzuri V, Krinsky V I and Pérez-Villar V 1993 *Phys. Rev.* E **48** R3232
[48] Muñuzuri A P, Innocenti C, Flesselles J M, Gilli J M, Agladze K I and Krinsky V I 1994 *Phys. Rev.* E **50** R667
[49] FitzHugh R 1961 *Biophys. J.* **1** 445